

Small angle light scattering option for AR rheometers

Aly Franck, TA Instruments, Germany

Keywords: SALS, simultaneous measurements, rheometry, interference, Rayleigh scattering, form factor, viscosity, structure changes

INTRODUCTION

When light travels through material, interactions with the electrons of the atoms or molecules change the properties of light. These changes are measured in an optical experiment. The results provide insight into the material's microstructure in terms of size, shape and orientation. When optical measurements are performed simultaneously with rheological experiments, alterations of the material's structure can be monitored and information to explain and better understand the rheology of flowing systems is obtained.

SALS is one method to probe the internal structure of materials. In a SALS experiment the spatial distribution of the intensity

of the scattered light of an incident light beam interacting with the material is measured. From the intensity pattern of the scattered light, changes of structure elements with a characteristic length scale in the order of the wavelength of light are observed.

Simultaneous SALS and rheological measurements on emulsions, suspension or similar structured systems provide structural information as a function of the applied shear rate or stress, important to interpret rheological flow phenomena such as shear thinning, shear thickening, shear banding, yield stress, etc..

PROPERTIES OF LIGHT

To explain the behavior of light in a scattering experiment, light is represented by an

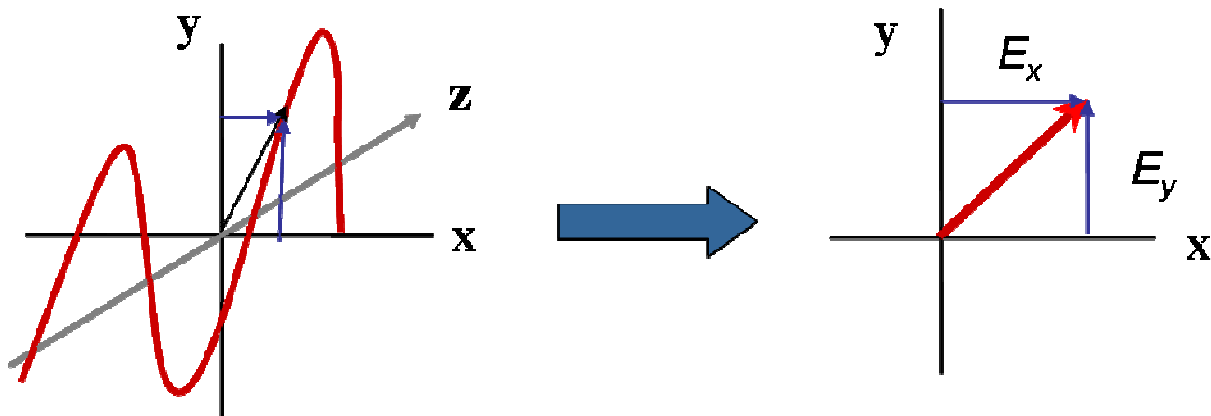


Figure 1: Representation of the electrical field \underline{E} propagating in space

electromagnetic wave, propagating in the z-direction through free space at the speed of light. An electromagnetic wave is a transverse wave with an electrical field \underline{E} characterized by two components in x and y direction, orthogonal to the direction of travel (Figure 1). The oscillation direction of the electrical field is referred to as polarization direction.

Background and definitions

The electrical field of the light \underline{E} propagating in positive z direction is represented in complex notation (see appendix):

$$\vec{E} = \vec{E}_o \exp\{i(kz - \omega t)\} \quad (1)$$

The components, \underline{E}_x and \underline{E}_y in x and y direction also describe a sinusoidal function according to:

$$\vec{E}_{x,y} = \vec{E}_{x_o,y_o} \exp\{i(kz - \omega t)\} \quad (2)$$

Introducing the refractive index n , which is defined as the ratio of propagation speed of light in the material and in vacuum, provides:

$$\vec{E}_{x,y} = \vec{E}_{x_o,y_o} \exp\{i\omega(nz/c - t)\} \quad (3)$$

The polarization of light is defined by the components \underline{E}_x and \underline{E}_y . Since the two components may have a different phase δ_x and δ_y , expression (3) can be formulated as:

$$\vec{E}_{x,y} = \vec{E}_{x_o,y_o} \exp\{i\omega(nz/c - t) + i\delta_{x,y}\} \quad (4)$$

When $\delta_x = \delta_y$, the light is linearly polarized. The oscillation direction of \underline{E} is the direction of polarization. When the phase of the components x and y changes differently when light travels through a material, the material is birefringent, when the ratio of the magnitudes $|E_x|$, $|E_y|$ changes, the material is dichroic.

Intensity of a light wave

Energy and momentum are transported by a wave. The energy for a transverse wave is

perpendicular to the propagation direction. For an elastic wave the sum of potential and kinetic energy is constant, no energy is dissipated and the change with time of the electric field vector \underline{E} is proportional to the angular frequency ω and amplitude \underline{E}_o .

$$\frac{d\vec{E}}{dt} = \omega \vec{E}_o \quad (5)$$

When dE/dt is maximum, all energy exists as kinetic energy is:

$$W = \frac{1}{2} \rho \left(\frac{d\vec{E}}{dt} \right)^2 \quad (6)$$

The energy propagates with the speed of light c in the direction z. The measured intensity I is:

$$I = Wc = \frac{1}{2} \rho \left(\frac{d\vec{E}}{dt} \right)^2 c = \frac{1}{2} \rho \omega^2 \vec{E}_o^2 c \quad (7)$$

The intensity is proportional to the square of the amplitude of the electric vector \underline{E} .

Spherical waves such as light propagate from the center in all directions equally; the intensity is distributed with increasing radius r over an increasing sphere surface – thus is proportional to $1/r^2$. Since $I \sim E^2$, the amplitude \underline{E}_o is inversely proportional to the distance r .

For a spherically propagating electric field, the wave equation reduces to:

$$\vec{E} = \vec{E}_o \frac{1}{r} \exp\{i(k\vec{r} - \omega t)\} \quad (8)$$

Interference and scattering

Coherent light consists of waves with a defined phase over a given distance (coherence length $\sim 1\text{m}$) and time, typically light originating from the same source.⁽¹⁾ When two coherent light waves meet in space, the magnitudes of the electric field vectors add up. When the maxima superpose, the amplitude doubles. The measured intensity, which is the square of

the magnitude increases by a factor 4. This is referred to as constructive interference. When maximum and minimum overlay in space, the amplitude i.e. intensity vanishes. This is destructive interference. Depending on the position in space, constructive and destructive interference alternate and the projection onto a screen shows an interference pattern with dark and white lines. Colors of the rainbow are visible because various wavelengths of the white light are filtered out as a result of interference. Light reflected from the top and bottom of a thin film also generates a typical line pattern as a result of interference.

Consider two coherent light sources with a distance d apart. Two coherent light sources can be obtained by orientating two mirrors in relation to a spot light and create two virtual light sources at the focal points with the distance d apart (Figure 2) ⁽¹⁾.

According to the Huygens principle, every point on the wave front is at the origin of a new elementary wave. The two focal points are the radiation center of two new coherent waves propagating in radial direction. The

waves overlap and show constructive or destructive interference depending on the location in space. The light projected on a screen at a distance D from the focal points shows a pattern of dark and bright lines (Figure 2a). Let P be the observation point on the screen at an angle φ and A and B the origin of the interfering waves. The light beam traveling along the path BP has a path difference in reference to the beam traveling through point A (Figure 3c). When the intensity at the observation point is maximum (P'') (constructive interference), the path difference ($BP-AP$) must be equal to a multiple of the wavelength. If the path difference B equals half the wavelength, the two light beams are 180 degrees out of phase (P'). The amplitudes add up and the intensity at the observation point P' cancels out.

All points with equal intensity can be found on a hyperbolic curve with $(PA-PB) = n\lambda$; $n=0, \pm 1, \pm 2, \pm 3, \dots$ (Figure 2b) The same phenomenon is observed when analyzing the light scattered by crystals. Sir William Henry Bragg and son Sir William Laurence discovered the relationship between diffraction angle and crystal (Lattice)

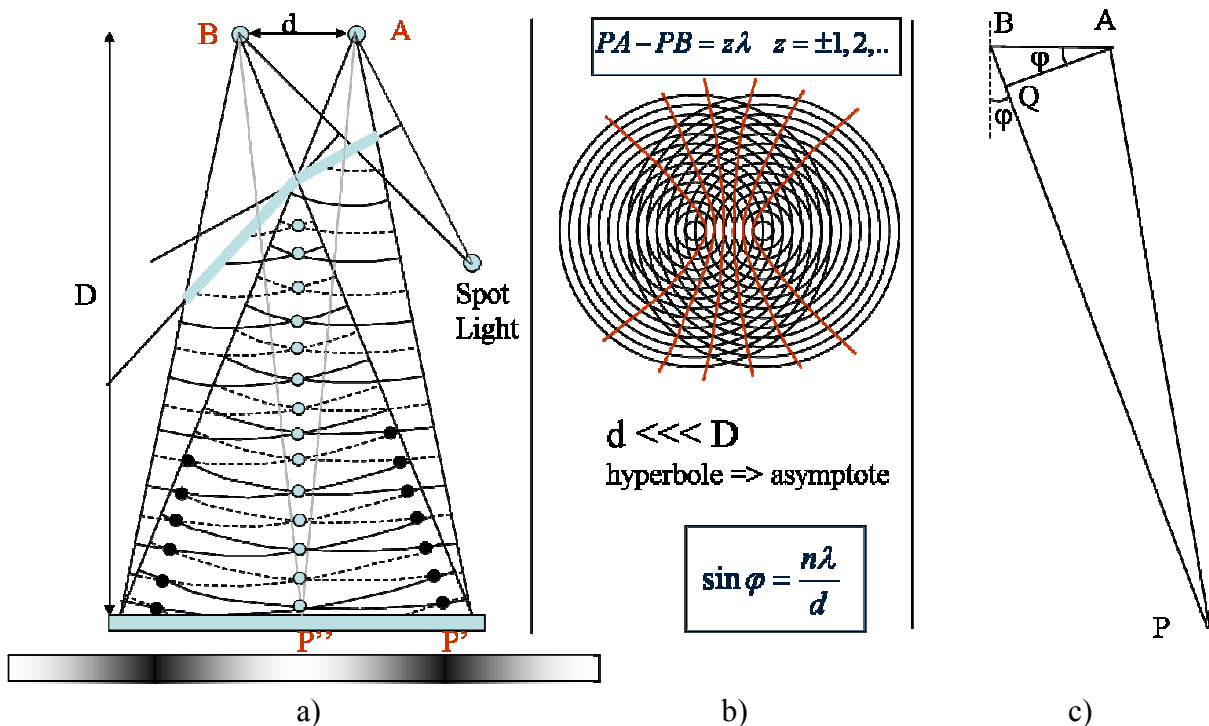


Figure 2: Interference of two coherent light beams

structure. They received the Nobel price in 1915 in recognition for the investigation of crystal structures by means of X-rays⁽⁹⁾.

When D (distance to screen) $\gg d$ (distance of scattering points), the observation points are far away from the scattering centers and the hyperbols can be approximated by asymptotes. For the triangle ABQ in figure 2c, the conditions for interference can be derived as:

$$d \sin \varphi = n\lambda \quad (9)$$

Constructive interference occurs when $n=1, \pm 2, \pm 3, \dots$ and destructive interference when $n=\pm 1/2, \pm 3/2, \dots$. The Bragg diffraction law relates the path difference to the object size. Diffraction of light can be used to analyze the structure in materials when the size of the structural objects is in the order of the magnitude of the wavelength of the light. However the diffraction pattern does not directly relate to the characteristic dimensions of an object – but provides the “number of wavelength that fit between scattering points of the object”⁽¹⁰⁾. As such the scattering pattern is a representation of the inverse image of the real space. When micro-structures in flowing systems are oriented, SALS provides information about size and shape of these objects. If these structures have the same size and are nicely spaced, interference patterns are visible. If the objects have different size, the typical interference patterns disappear and the scattered light produces an irregular diffraction (scattering) pattern.

SMALL ANGLE LIGHT SCATTERING THEORY

When light intercepts an obstacle like a particle, molecule, etc. it will emit a scattered wave. Coherent scattering occurs when the secondary wave oscillates in phase with the primary (incident) wave. The

measurement of the amplitude & polarization properties of the scattered light at various angles relative to the incident light beam provides structural information about the material.

In a SALS experiment the light intensity and not the amplitude of the electric field vector is measured. The intensity of a wave is proportional to the square of the amplitude $|\underline{E}|^2$.

The scattered intensity at the screen is proportional to the incident intensity and scales with the square of the distance from the scattering center.^(2 page 12) according to:

$$I_s = \frac{I_i F(\theta, \phi)}{k^2 r^2} \quad (10)$$

$F(\theta, \phi)$ is a dimensionless function and depends on the orientation of the scattering object with respect to the incident wave and its polarization state.

Rayleigh scattering⁽⁵⁾

As long as scattering objects in a medium are smaller than $\lambda/20$, the scattering can be approximated by dipole scattering (Rayleigh scattering). The electromagnetic interactions of the light with matter displace the electrons of a molecule in reference to the nucleus and produce an oscillating dipole which emits a new light wave, the secondary wave. The dipole P is related to the electromagnetic field E according to:

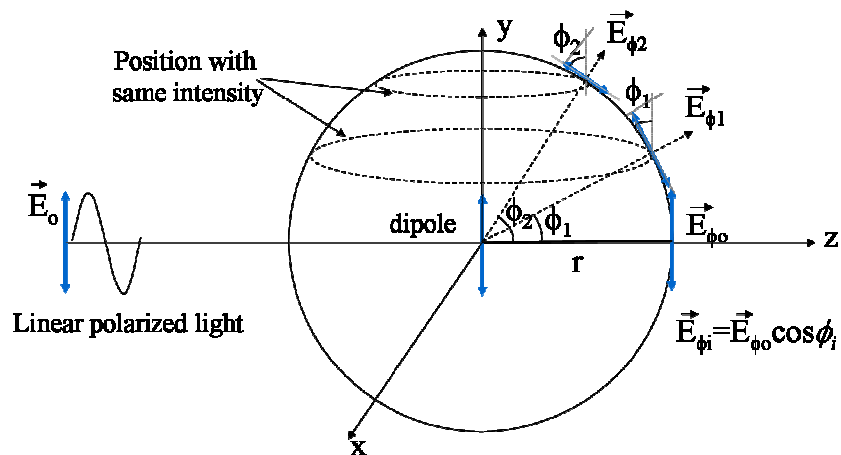


Figure 3: Dipole scattering of linear polarized light

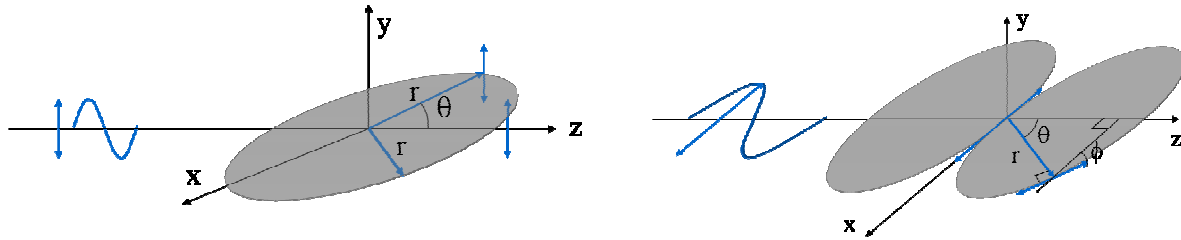


Figure 4: a) Dipole scattering of vertical polarized light b) ..of horizontal polarized light

$$\vec{P} = \alpha \vec{E} \quad (11)$$

with α the polarizability of the molecules. The emitted energy of an oscillating dipole I_s is proportional to the square of the averaged second derivative of the dipole moment⁽⁵⁾ (Theory of an oscillating dipole);

$$I_s = \frac{2}{3c^3} \left\langle \left| \frac{d^2 \vec{P}}{dt^2} \right|^2 \right\rangle \quad (12)$$

c is the speed of light. The intensity of the incident light I_i is proportional to the square of the amplitude E_o ^(2 page 64).

$$I_i = \frac{c}{8\pi} E_o^2 \quad (3)$$

With

$$\vec{E} = \vec{E}_o \cos(2\pi ft) \quad (4)$$

the intensity of the emitted light is:

$$I_s = \frac{2c}{3c^3} 8\pi^4 f^4 \alpha^2 E_o^2 \quad (5)$$

Inserting equation (13) and replacing c/f with the wave length, following expression for the scattered light intensity is obtained:

$$I_s = \frac{8}{3} \pi I_o k^4 \alpha^2 \quad (6)$$

The intensity of the scattered wave is proportional to the intensity of the incident wave and the 4th of the power of the wave length.

Theoretically the intensity I_s could be measured from the extinction of the incident light in direction of propagation. However the extinction is too small, therefore

the scattered light has to be measured directly. Since light scatters in all directions, the intensity at the surface of a sphere around the scattering center needs to be measured.

When the incident light is linearly polarized with the polarization direction in y direction, the induced dipole at the scattering origin oscillates in the same plane and radiates light waves in all directions, perpendicular to the oscillation direction with an amplitude depending on the polarizability α (Figure 3).

Figure 3 shows two examples of scattered waves in the yz plane at a distance r from the scattering center. With ϕ , the angle between the oscillation direction of the incident and the scattered light, the magnitude of the electrical vectors of the scattered light can be expressed as:

$$\vec{E}_{\phi_i} = \vec{E}_{\phi_o} \cos \phi_i \quad (17)$$

ϕ_i refers to the angle of the scattered wave i , ϕ_o to the scattered wave in propagation direction of the incident wave. With the intensity being the square of the amplitude of the electrical vector, the expression for the intensity can be formulated :

$$I_{\phi_i} = I_{\phi_o} \cos^2 \phi_i \quad (18)$$

The intensity is perpendicular to the direction of oscillation i.e. the polarization direction. The dashed circles in figure 3 represent trajectories on the sphere surface with constant intensity

The total scattered intensity is the intensity of the scattered light in all directions.

Integration of the intensity over all surface elements on the sphere surface provides the total surface intensity:

$$I_s = \frac{8}{3} \pi r^2 I_{\phi_0} \quad (19)$$

Because of the polarization properties of light, three states for the polarization of the incident light are possible, vertical, horizontal and not polarized.

Since the intensity measurements on the SALS instruments are made in the xy plane, the angle ϕ is replaced with the observation or scattering angle θ .

For vertical polarized incident light, the electrical field oscillates in the direction y (Figure 4). For all angles θ in the xz plane, the angle ϕ in the zy plane is 0° . That means $\cos\phi=1$ and $I_{\theta,v}=I_{\phi_0,v}$. The scattering intensity for all angles in the xz plane is the same. (v refers to vertical polarized light)

For horizontal polarized light, the electric field vector oscillates in the direction of the x axes. The angle θ in the xz plane is equal to the angle ϕ and $\cos\theta = \cos\phi$. The intensity for all angles θ in the x-z plane is $I_{q,h}=I_{\phi_0,h} \cos^2\theta$. (h refers to horizontal polarized light)

For unpolarized light, the intensities in vertical and horizontal direction add up and the intensity for any angle θ is:

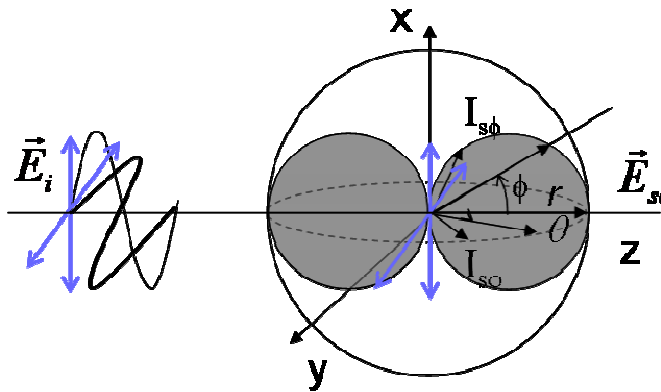


Figure 5: Intensity for Rayleigh scattering of vertical and horizontal polarized light.

$$I_\theta = I_{\phi_0} \frac{1 + \cos^2 \theta}{2} \quad (20)$$

Note that for $\theta = \pi/2$, the scattered intensity for horizontal polarized light is zero ($\cos(90^\circ)=0$). Therefore vertical polarized light is typically used in SALS experiments. Figure 5 shows the intensity of vertical and horizontal polarized light in all directions. The intensity for vertical polarized light at a fixed angle θ is constant in all directions as represented by the dashed circle in figure 5. Constant intensity for horizontal polarized light at all angles is the surface of a spindle torus with the scattering dipole at the center.

Combination of the equations (16), (19), and (20) leads to the equation for the scattered intensity for any angle θ as a function of the incident light intensity I_i

$$I_s = \frac{(1 + \cos^2 \theta) k^4 |\alpha|^2}{2r^2} I_i \quad (21)$$

The angular distribution of Rayleigh scattering of non-polarized light is governed by the term $(1 + \cos^2(\theta))$ and is symmetric in the plane normal to the incident direction of light (plane of the 2D detector in a SALS experiment). Maximum scattering occurs for $\theta=0$, minimum for $\pi/2$.

Since the molecules are closely packed, dipole scattering dominates and phase differences between light waves emitted from the same molecule are small and negligible. ⁽⁴⁾

Rayleigh Debye scattering

When the objects become comparable or larger than the wave length ($a \gg \lambda/20$), light scattering from elements internal to the object occurs and the phase difference between the emitted light waves is not negligible anymore. Assuming the refractive index of the solvent and the object is approximately the same, only contributions to the

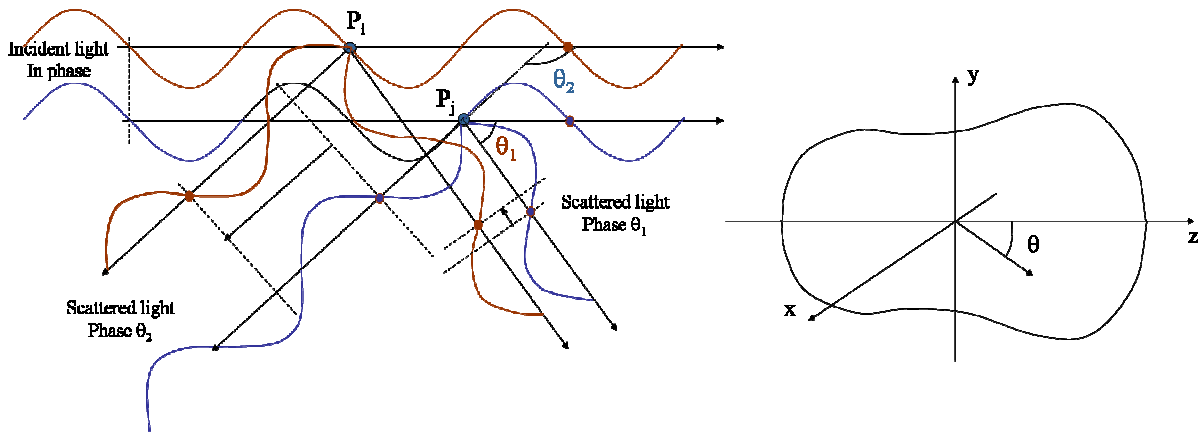


Figure 6 a) Scattering showing constructive and destructive interference $\lambda > (P_j - P_i) > \lambda/2$
 b) intensity as a function of the scattering angle θ if distance $(P_j - P_i) < \lambda/2$

scattering objects must be accounted for. As the scattering angle θ deviates from 0° , the phase difference increases and destructive interference occurs (Figure 6a). No phase difference nor destructive interference is obtained for $\theta = 0^\circ$. As long as the object dimensions are not exceeding $\lambda/2$, the scattering intensity decreases smoothly with increasing scattering angle. (Figure 6b)

For larger particles, the intensity distribution shows maxima and minima, related to the phase difference i.e. size of the object. The difference in phase between the incident and the scattered wave vectors is described by the scattering vector ⁽³⁾

$$\vec{q} = \vec{k}_i - \vec{k}_s \quad (22)$$

For the process where light is scattered by 2 elements on the object, the elements sepa-

rated by the vector \underline{x} , the phase difference δ between the scattered light in direction $\underline{k}_s = k\underline{n}_s$ and the incident light $\underline{k}_i = k\underline{n}_i$ is given as (Figure 7):

$$\delta = kl_2 - kl_1 = (\vec{k}_s - \vec{k}_i) \cdot \vec{x} = \vec{q} \cdot \vec{x} \quad (23)$$

The magnitude of the scattering vector is (see appendix 2)

$$|\vec{q}| = 2k \sin\left(\frac{\theta}{2}\right) = \frac{4\pi \sin\left(\frac{\theta}{2}\right)}{\lambda} \quad (24)$$

The phase difference of the scattered light from the object in any direction is referenced to a common origin and the complex amplitudes are summed up in the phase factor $e^{i\delta}$. The scattering of the entire object is the integral of the phase factor over the object volume according to ⁽³⁾:

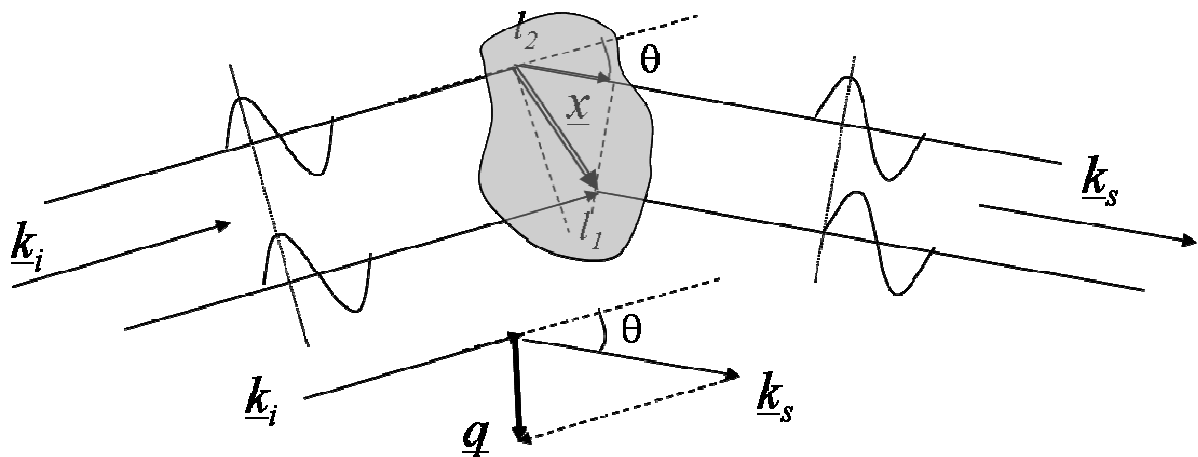


Figure 7: Rayleigh-Debye scattering

$$R(\theta, \phi) = \frac{1}{V} \int_V e^{iqx} d\vec{x} \quad (25)$$

$R(\theta, \phi)$ is the Rayleigh form factor. The amplitude of the scattered wave is the scattered amplitude of the pure Rayleigh scattering multiplied with the form factor $R(\theta)$ which is independent of polarization. The intensity of the scattered light is found by multiplying the intensity of Rayleigh scattering with $|R(\theta)|^2$. For incident unpolarized light, the scattered intensity is given as:

$$I_s = \frac{(1 + \cos^2 \theta) k^4 |\alpha|^2}{2 r^2} |R(\theta)|^2 I_i \quad (26)$$

Interference effects of large particles are taken into account through the form function $R(\theta)$. For the scattering angle $\theta=0$ (in direction of propagation), the form factor $R(\theta)=1$. According to Debye, the form factor can be expanded in a series according to⁽⁵⁾:

$$R(\theta) = 1 - a_1 \sin^2\left(\frac{\theta}{2}\right) + a_2 \sin^4\left(\frac{\theta}{2}\right) \dots \quad (27)$$

For small q , only the first two terms are important and $R(\theta)$ only depends on a_1 .

The form factor can be determined for many geometries. For example, the form factor for spheres with radius a can be expressed as a function of q :

$$R(q, r) = \frac{3}{(qa)^3} [\sin(qa - qa \cos(qa))] \quad (28)$$

The form factor R^2 as a function of the dimensionless scattering vector qa for monodisperse spheres shows a spherical symmetric scattering pattern with a central point, circumscribed by rings with intensity minima located at the roots of $R(\theta)=0$. From the location of the first minimum, the size of the scattered sphere can be obtained. Polydispersity of the beads removes the appearance of the minimum.

NB: Scattering of monodisperse beads (3 microns) is used to calibrate the pixels of the camera array for the scattering angle i.e. q value.

SALS OPTION

Design

The TA-SALS module for the AR series of rheometers is a compact, fully integrated option consisting of a lower Smart SwapTM assembly with the laser incorporated into a Peltier plate and an upper optical analysis assembly to collect the scattered light and to record the scattering image with a digital camera. The incident light is generated by a 0.95mW diode laser with a beam diameter of 1.1mm and a wave length of 635nm (Figure 9a).

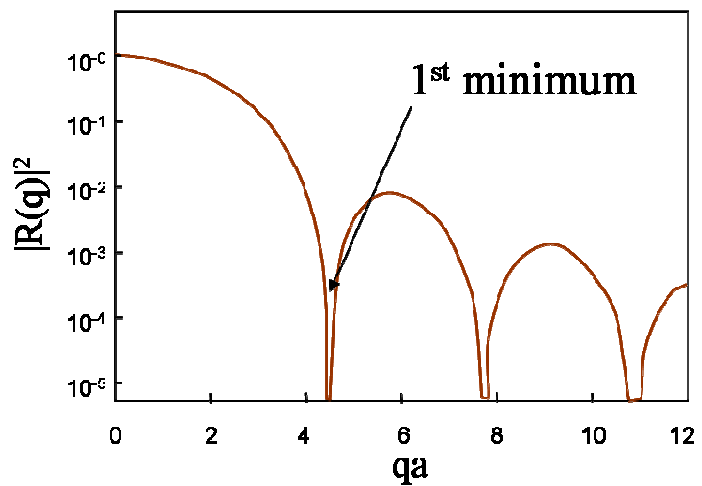
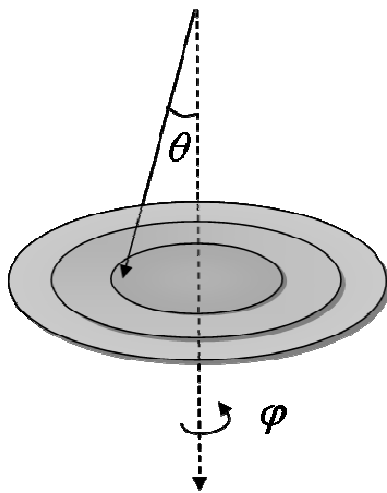


Figure 8: Form factor $R^2(q)$ for monodisperse beads

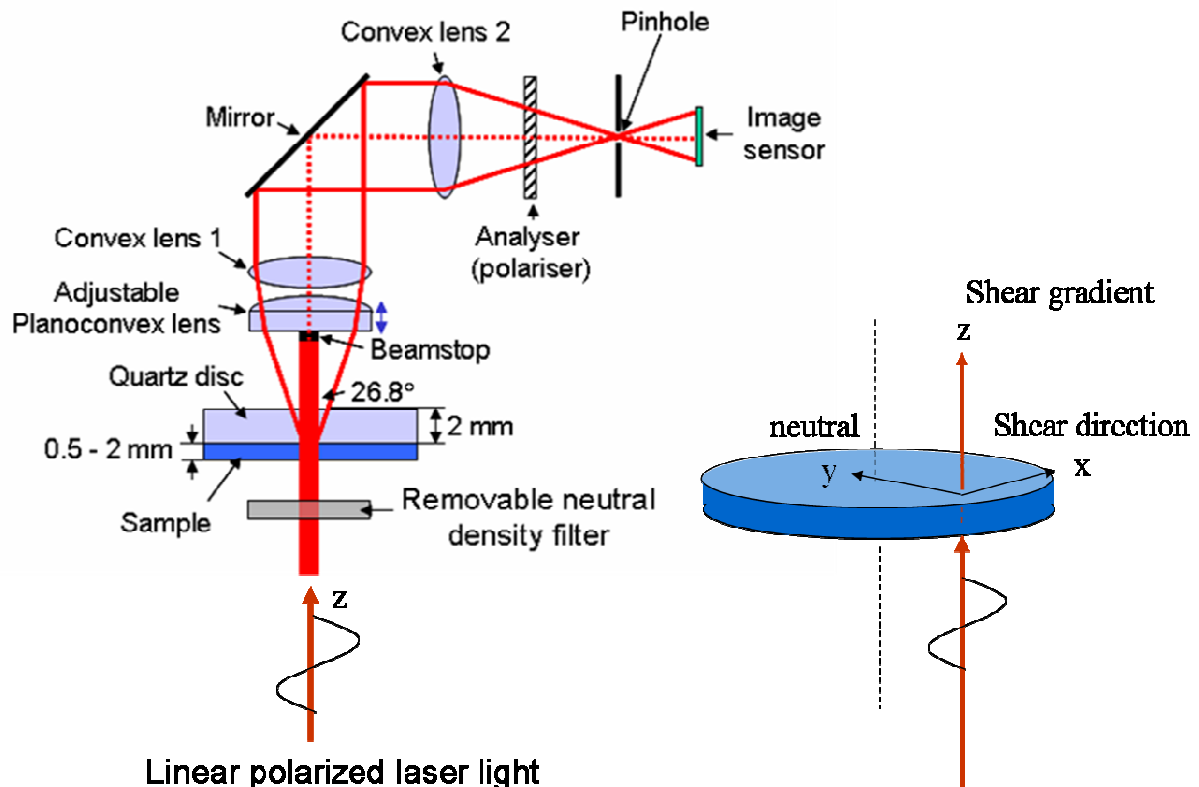


Figure 9: a) Schematic of the SALS setup b) Orientation of the laser in reference to the shear direction

The upper geometry is a 50mm plate of optical quartz glass ($n=1.457$ at 635 nm). The laser beam is located at $0.76 \times$ plate diameter i.e. 19 mm from the axis of rotation of the plate⁽⁶⁾. The laser (Figure 9b) beam is oriented in the direction of the shear gradient and the polarization of the incident light in shear direction

Because of the limited space above the upper plate, a mirror deflects the scattered image in an angle of 90° onto a 2D optical sensor. The effective area is $6.6 \times 5.3 \text{ mm}$ i.e. 1280×1024 pixels.

The laser produces linear polarized light, with the polarization direction pointing in shear direction. The optical setup provides a q range from 1.38 to $6.11 \mu\text{m}^{-1}$ (i.e. a scattering angle from 6 to 26.8°). This corresponds to a length scale of 1 to $4.6 \mu\text{m}$ (using Bragg law $d = \lambda / 2 \sin(\theta/2)$).

A pinhole in front of the camera is set at the focal point for the laser light used, such that divergent and convergent light will not pass through to the 2D array. The scattering

information from the focal point in the sample will be imaged onto the optical sensor. The focal point can be adjusted (plan convex lens) to be in the mid section of the sample, between Peltier plate and upper glass plate.

A neutral density filter allows adjusting the intensity of the initial laser light. A polarizer is placed in front of the pinhole and can be set too parallel or perpendicular polarization.

Calibration

Most of the time SALS images are used to evaluate the anisotropy in the sample and to follow the structural changes inferred by the deformation (rate) applied by the rheometer. The scattering experiment provides qualitative information to explain and understand the simultaneously measured rheological response. For a quantitative evaluation of the scattered intensity as a function of the scattering angle, the optical setup needs to be calibrated.

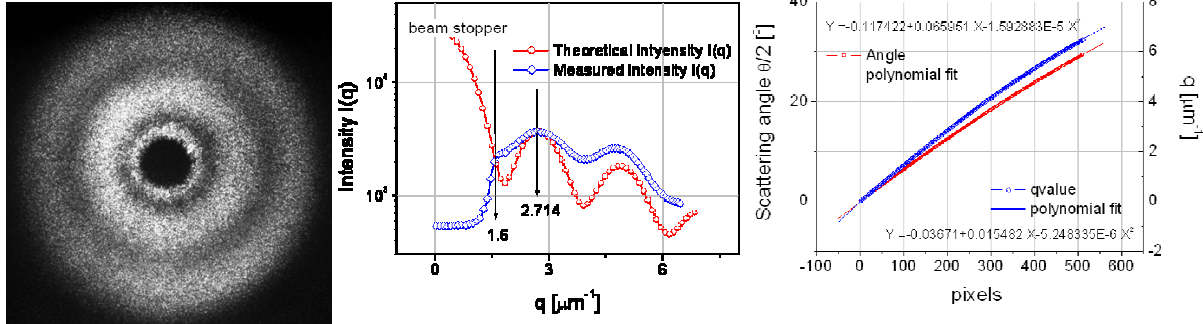


Figure 10: a) Mie scattering for 3 μm monodisperse PS spheres in water b) Theoretical Mie scattering calculated using the public domain program available at www.piliphaven.co/mieplot.htm c) calibration function for scattering angle i.e. q value with pixel position

In a first step, the scattering angle has to be related to the pixel position on the 2D sensor of the camera. Next the measured intensity needs to be corrected for the flatness of the sensor array.

In order to relate the scattering angle with the pixel position, the scattered intensity pattern of a well characterized sample is measured. The experimental and theoretical results are correlated to determine the calibration factor. The calibration sample used is a dilute dispersion of 3 μm monodisperse PS beads in water. The beads size is well within the characteristic length scale range of the SALS setup. The scattering of light at independent monodisperse beads of 3 μm provides a characteristic Mie scattering pattern and can theoretically be predicted. The pattern of the scattered light consists of a series of concentric rings of lower and higher intensity around the scattering origin (Figure 10a). Note, the Mie scattering pattern is also used to align the optical system by adjusting the orientation and position of the upper assembly.

Figure 10b shows a comparison of the theoretical and measured scattering intensity as a function of the scattering vector q . The theoretical values are calculated for a particle size of 3 μm , a wavelength of 635 nm and a refractive of 1.59 for the spheres and 1.332 for the water. q -value and scattering angle are related $q = 4\pi n / \lambda \sin(\theta/2)$; n is the refractive index of water. Figure 10c shows the calibration values for the scattering angle θ i.e. the q -vector.

The intensity measured at each individual pixel depends on the distance from the scattering center and the angle at which the scattered light beam hits the sensor (sensor surface is flat and not spherical). The flux of photons on the fixed pixel surface is inverse proportional to the square of the distance

$$D^2 = d^2 / \cos^2 \theta \quad (29)$$

with d the distance between scattering center and the sensor plate, in normal direction and D the distance between the scattering center and the measured pixel. The correction of the intensity for the oblique orientation of the flat screen is

$$I_{\text{obliq}} = I_m / \cos \theta \quad (30)$$

The corrected intensity I_{corr} is therefore

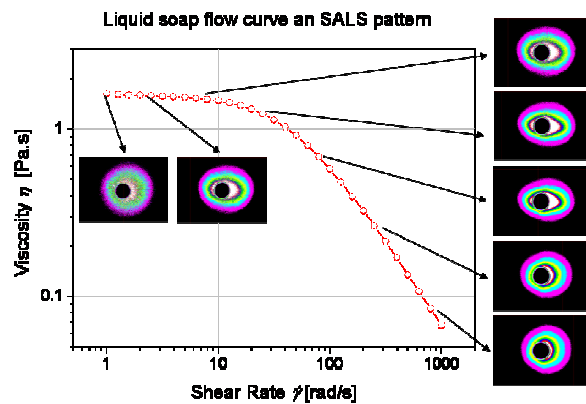


Figure 11: Steady Shear Viscosity as a function of shear rate. SALS scattering pattern suggest an alignment (shear banding) in flow direction at low shear rate followed by a structure reorientation i.e. break-up above 200 s^{-1} .

$$I_{corr} = \frac{I_m}{\cos^3 \theta} \quad (31)$$

with I_m , the experimental intensity.

The measured intensity corrected for the setup imperfections has been shifted vertically in figure 8b) to force the maxima of the first peak to overlap. As can be seen, the calibration of the intensity is less accurate as the second peak and the minima do not overlap. This has to do primarily with the remaining polydispersity of the “monodisperse” dispersion and optical imperfections of the SALS setup.

TEST RESULTS AND APPLICATIONS

Liquid soap in steady shear

A commercial liquid soap has been tested in steady shear at ambient temperature over a shear rate range from 1 to 1000 s^{-1} . The SALS images have been recorded to monitor structural changes in the material with increasing shear rate. In figure 11, the viscosity remains constant up to a shear rate of 10 s^{-1} and then drops by more than one decade at a shear rate of 1000 s^{-1} (shear thinning). The scattered intensity is low and shows a spherical symmetric pattern at the beginning. With increasing shear rate, the pattern becomes non-symmetric and extends in the vorticity direction. At the same time the scattered intensity increases. An orientation of structural elements (shear

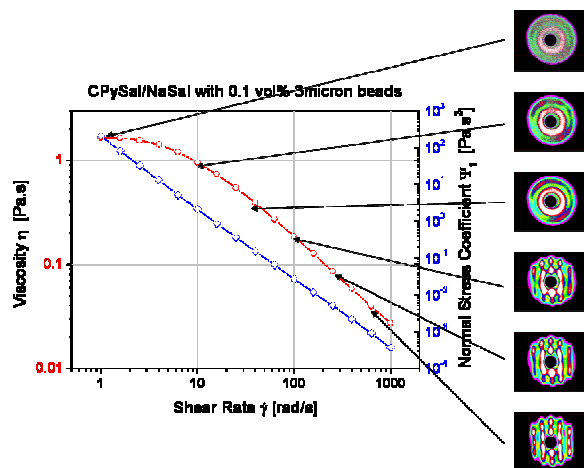


Figure 12: Steady Shear viscosity with pronounced

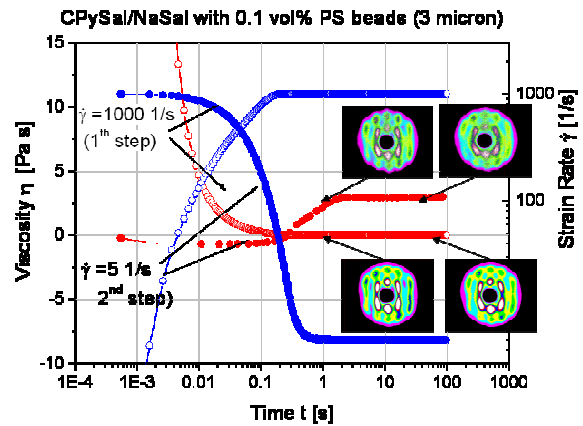


Figure 13: Two step shear rate experiment with a low rate (5 1/s) following a high rate (1000 1/s) steady shear zone. The induced structure decays slowly because it is stabilized by the viscoelastic nature of the micellar matrix.

banding?) in flow direction can be assumed. At 200 s^{-1} the pattern returns to spherical symmetry. The scattering pattern slightly elongates in flow direction when the shear rate approaches 1000 s^{-1} . Above 200 s^{-1} , structural reorientation resp. structure break-up takes place while the viscosity function continues to behave highly shear thinning.

Alignment of particles in a micellar solution under steady shear

A dispersion of 3 μm PS beads (0,1 vol%) in a micellar solution (CPySa 100mMol, NaSal 50mMol) has been prepared. The dispersion was loaded carefully into the rheometer, taking care to avoid the enclosure of air bubbles. Steady shear tests in a shear rate range from 1 to 1000 s^{-1} at 25°C have been performed (Figure 12). Beyond the short plateau region, the viscosity exhibits extensive shear thinning over two decades in viscosity. Images of the SALS patterns were recorded at various shear rates. The SALS pattern show spherical symmetry with two intensity minima at low shear rate. These minima are typical for the scattering of the independent evenly distributed 3 μm particles. In the viscoelastic fluid, these particles align into strings above a critical shear rate of 100 s^{-1} . The 6-fold symmetry observed in the scattering pattern

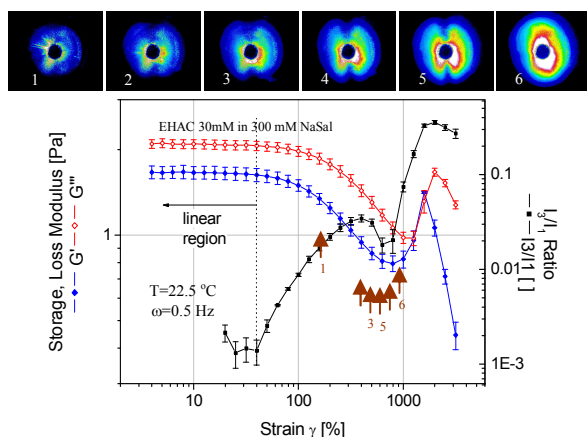


Figure 14: LAOS measurements in a strain amplitude range from 10 to 3000%. The transition into the non linear regime, showing a maximum in the loss modulus and the higher harmonic stress contributions is associated with a significant structural re-

is indicative for a hexagonal close packed crystalline order (possibly at the walls)⁽⁷⁾. The scattered intensity image suggests an aligned string phase, ordered as a crystalline hexagonal packing structure.

When the flow stops, the scattering pattern does not return to the original spherical symmetry, the fluid retains the hexagonal crystalline order as shown in figure 13. The fluid is ordered during a steady shear flow at 1000 s^{-1} . After 100s the shear rate is stepped down to 5 s^{-1} . Although the scattering intensity is reduced, the 6-fold symmetry is conserved for a long time.

The viscosity recovers within 1-2 seconds and reaches a steady state value of 3 Pa.s. This is approximately double of the viscosity compared to steady shear in the un-oriented state (Figure 13). It takes more than one hour continuous shear at low rate to recover the original structure. The viscoelastic nature of the micellar solution prevents the stringing of the particles at low rate in the suspension at equilibrium and at the same time slows down the break-up of the previously induced structure.

Shear induced phase separation of micellar solutions in LAOS

RheoSALS measurements were performed on a 40mMol EHAC solution in

300mMol NaSal at 25 °C. EHAC is a cationic surfactant (erucyl bis-hydroxyethylmethylammonium chloride) which forms wormlike micelles in the presence of the hydrotropic salt sodium salicylate. This system is known to exhibit shear-induced phase separation when a sufficient high shear stress is applied⁽⁸⁾

Oscillation experiments in the strain range from 0.1 to 30 were performed at ambient temperature and the transition from linear to non-linear behavior monitored by evaluating the stress response and the scattering pattern (Figure 14). Below a strain amplitude of 100%, the system behaves linear viscoelastic and no scattering is observed. Between 100 and 500% strain, the dynamic moduli G' and G'' decrease slightly with a small contribution of the third harmonic stress. The material system shows inherent non-linear behavior as the material is strained to its maximum. Around 500% strain the scattered intensity shows formation of a “butterfly” pattern. Beyond this strain, G' drops significantly, G'' goes through a maximum as well as the 3rd, 5th, 7th and 9th harmonic stress contributions. The scattered intensity develops a strong butterfly pattern, suggesting a strong anisotropy perpendicular to the flow direction, which probably results from phase separation⁽⁸⁾ where interfaces between the two phases develop in the flow-vorticity plane.

CONCLUSION

A compact SALS option has been developed for use with the AR series of rheometers. The option is designed for fast setup and minimum optical adjustment. For quantitative analysis, the SALS option has to be calibrated using a diluted dispersion of $3 \mu\text{m}$ spheres in water.

Application examples of simultaneous rheological SALS measurements are presented to demonstrate how SALS measurements can be used to complement the rheological measurement when investigating material structure changes in steady and oscillation flows.

References

1. H. Vogel „Gerthsen Physik“ 20 Auflage (1999) Springer Verlag Berlin, Heidelberg, New York. ISBN 3-540-65479-8
2. H.V. van de Hulst „Light scattering by small particles“, Dover publications, Inc. New York (1981) ISBN 0-486-64228-3
3. G. Fuller “Optical rheometry of complex fluids”, Oxford University Press, New York, Oxford, (1995) ISBN 0-19-509718-1
4. W. Weizel “Einführung in die Physik” 5te Auflage Band 3. Optik und Atomphysik B.I.Hochschultaschenbuecher, Bibliographisches Institut Ag, Mannheim
5. J.Springer „Einführung in die Theorie der Lichtstreuung verdünnter Lösungen großer Moleküle, published by Applied Research Laboratories (1970)
6. Carvalho, M.S., Padmanabhan, M., Macosko, C.W. J.Rheol. 38, 1925 (1994)/
7. Scirocco, R., Vermant, J., Mewis, J., J. Non-Newtonian Fluid Mech. 117, 183 (2004).../
8. private communication Norm Wagner Matt Liberatore
9. http://nobelprize.org/nobel_prizes/physics/laureates/1915/present.html
10. http://en.wikipedia.org/wiki/Bragg%27s_law#Reciprocal_space

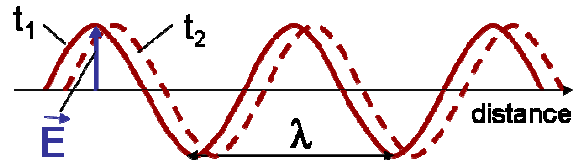


Figure 1a: Wave as a function of distance.

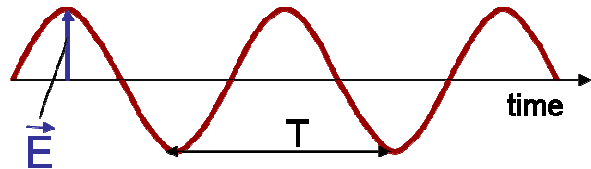


Figure 1b: Wave as a function of time

APPENDIX 1 PROPOGATION OF WAVES

Consider a perturbation such as a sinusoidal deflection propagating along a path z as a function of time (for example a continuous deflection along a rope).

A snapshot (Figure 1a) at a fixed time t_1 shows a sinusoidal trace along the direction z . The distance from peak to peak is the wave length and represents the distance covered over one cycle of oscillation. An instant dt later, the wave form has moved the distance vdt along the axes z ; v being the speed of propagation.

The same wave can be monitored as a function of time at a fixed position x_0 ; the deflection describes a sinusoidal waveform as a function of time (Figure 2b). The time between two peaks is the period of oscillation and represents the time elapsed during one cycle of oscillation. The inverse of the period $1/T$ is the frequency in Hz and represents the number of oscillation cycles per unit of time^(1,3,4). Assuming $y=f(x,t)$ to be a simple deflection at the position x at time t . The deflection starts at time $t=0$ at the posi-

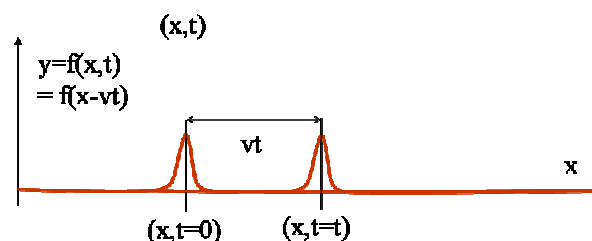


Figure 2: Propagation of a deflection along a path x

tion x and propagates along the path x with the propagation speed v . At a time t , the deflection can be found at the position $x+vt$ from the start position x at time $t=0$.

Time and position for a propagating wave are related, which means, that $f(x,t)$ does not independently depend on x or t , but on the combination of both. At a time t_1 , the deflection y_1 at position x_1 is the deflection at position x_0 at time t_0 i.e.
 $y_1=f(x_1,t_1)=f(x_1-vt_1)$.

For $y=f(x-vt)$ the wave propagates from left to right, alternatively for $y=f(x+vt)$ the wave propagates from right to left along the direction x . $(x-vt)$ is the phase of the wave.

The plane perpendicular to the direction of propagation for all waves with $(x-vt)=\text{constant}$ is referred to as “wave front”. (Figure 3) Waves propagating on a linear path are plane waves, their wave fronts are parallel planes. Waves propagating from a center point in all directions are spherical waves and their wave fronts are spheres.

When the oscillation of the wave is perpendicular to the propagation, the wave is a transverse wave – electromagnetic waves are transverse waves. Waves oscillating in the direction of propagation are longitudinal waves (spiral spring or sound waves).

Transverse waves can be represented by a vector with two components in the x,y plane, perpendicular to the propagation direction z , defining the direction of polarization. Longitudinal waves are not polarized.

The speed of propagation v divided by the distance travelled during one cycle (wave length λ) represents the number of cycles

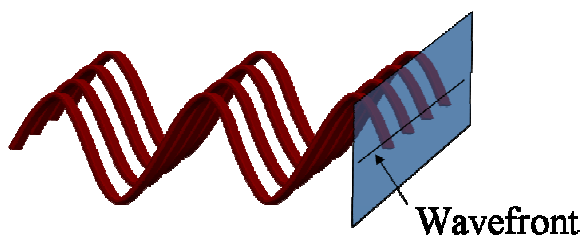


Figure 3: The wave front of plane waves propagating

per time, this is the frequency f in Hz.

$$f = v/\lambda$$

With $f=\omega/2\pi$ (ω angular frequency) the wave length can be expressed as:

$$\lambda = 2\pi v/\omega$$

Similar to the frequency ω , which represents the number of cycles/ unit of time, does the wave number k represent the number of cycles/distance. k is the wave number and related to the frequency and the speed of propagation according to:

$$k = \omega/v = 2\pi f/v = 2\pi/\lambda$$

A harmonic wave oscillates according to a sinusoidal function. At a given time t in space under steady state oscillation, the deflection is described as:

$$y=y_0\sin(kx)$$

The profile of a sinusoidal function repeats after a distance $x=2\pi/k=\lambda$. The general equation for an oscillating wave at a point z on the propagation axes is:

$$y=y_0 \sin(\omega t + \varphi)$$

If $t=0$ at a position z , then $\varphi=kz$ and above wave equation reduces to:

$$y = y_0 \sin(\omega t + kz)$$

in complex notation

$$y = y_0 e^{i(\omega t + kz)}$$

Light waves are electromagnetic waves and are represented by the electric field $\underline{E}(t,z)$ propagating in direction z at the speed of light $c=\omega/k$. The equation of motion for the electric field vector is:

$$\underline{E}=\underline{E}_0 \exp\{i(kz-\omega t + \varphi)\}$$

The sign of the argument is a matter of convention.

Since a wave propagates along a direction

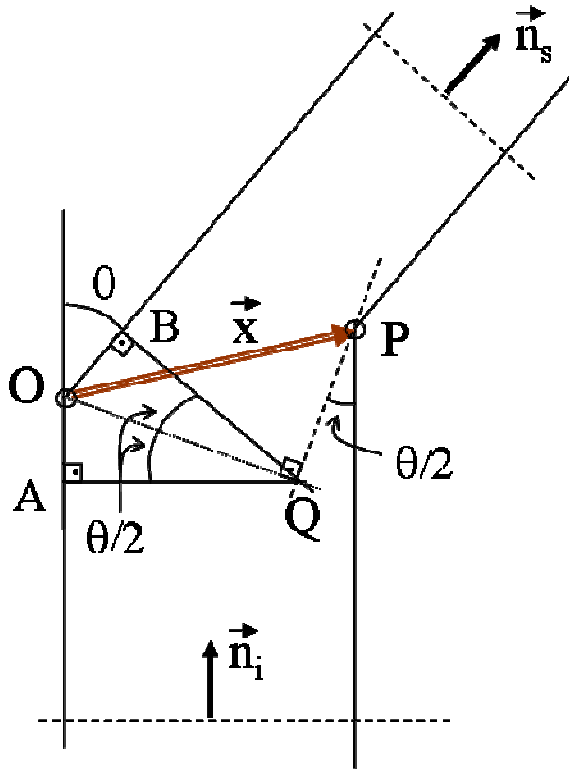


Figure 4: Determination of the q vector

z in space (light propagates radial from a center point into all directions), k is a vector and not a scalar value.

With n , the refractive index defined as c/v , the ratio of speed of light in vacuum and speed of light in matter, the wave number k can be expressed as:

$$k = \frac{2\pi n}{\lambda}$$

APPENDIX 2: DETERMINATION OF THE MAGNITUDE OF THE Q-VECTOR

The phase factor $e^{i\delta}$ represents the interference effects of the scattered waves and depends on the scattering angle θ and the distance $d = |\underline{x}|$ between the scattering points of the object.

Consider coherent light travelling along the direction \underline{n}_i and scattered by an object with a characteristic length scale \underline{x} in the direction \underline{n}_s .

$OQ = b$ is the bisectrix of the angle AOB .

With the scattering angle θ , and OQ the bisectrix, the angle $AOQ = (180-\theta)/2$. Consequently the angle $AQO = 180-(180-\theta)/2-90 = \theta/2$. The distance $OA = OQ \sin(\theta/2) = b \sin(\theta/2)$.

The total path difference between a ray passing through O and P is:

$$\begin{aligned} AO + OB &= 2OA = 2b \sin(\theta/2) \\ &= (\underline{n}_s - \underline{n}_i) \cdot \underline{x} \end{aligned}$$

The phase difference δ is obtained by multiplying the path difference with $k=2\pi/\lambda$:

$$\delta = \frac{4\pi}{\lambda} b \sin \theta/2 = k \cdot (\underline{n}_s - \underline{n}_i) \cdot \underline{x} = (\underline{k}_s - \underline{k}_i) \cdot \underline{x} = \underline{q} \cdot \underline{x}$$

In the plane PQ , perpendicular to OQ , the path difference is the same. The form factor therefore is obtained by integrating the phase factor along the bisectrix by slices of thickness db and an area B : ^(2 page 87)

$$R(\theta) = \frac{1}{V} \int_{-\infty}^{\infty} B e^{ikb2 \sin \theta/2} db$$